Mol Neurobiol
DOI 10.1007/s12035-015-9222-2

Overexpression of Fibulin-5 Attenuates Ischemia/Reperfusion Injury After Middle Cerebral Artery Occlusion in Rats

Jia Guo[1] · **Chuang Cheng**[1] · **Cindy Si Chen**[2] · **Xiangfeng Xing**[1] · **Guanghui Xu**[1] · **Jinzhou Feng**[1] · **Xinyue Qin**[1]

Received: 14 March 2015 / Accepted: 21 May 2015

Abstract Ischemia/reperfusion (I/R) injury after middle cerebral artery occlusion (MCAO) induces detrimental processes such as oxidative stress, inflammation, and apoptosis. All parts of the neurovascular unit are involved in these pathological processes. Fibulin-5 is a 66-kD glycoprotein secreted by various vascular cells, including vascular smooth muscle cells (SMCs), fibroblasts, and endothelial cells. As an extracellular matrix protein involved in cell adhesion, fibulin-5 has been widely studied in tumor growth and invasion. However, the effects of fibulin-5 on brain injury following ischemia/reperfusion have not been reported. In this study, we examined the effect of overexpressed fibulin-5 on reactive oxygen species (ROS) production. Fibulin-5 overexpression attenuated ROS expression, which in turn decreased apoptosis and blood–brain barrier (BBB) permeability following MCAO and reperfusion. Fibulin-5 also improved neurological deficits but had no effect on infarction volume. T2-weighted MRI and electron microscopy further confirmed brain edema reduction and decreased BBB disruption in fibulin-5 overexpression recombinant adenovirus (Ad-FBLN) treated rats. In addition, tight junction protein occludin was significantly degraded and matrix metalloproteinase 9 (MMP-9) immunoreactivity was significantly increased. Fibulin-5-mediated ROS decrease was not due to increased total superoxide dismutase levels but was instead correlated with the activation of Rac-1 pathway. The findings highlight the importance of antioxidant mechanism underlying cerebral ischemia/reperfusion.

Keywords Fibulin-5 · Ischemia/reperfusion · ROS · Rac-1 · Apoptosis · Blood–brain barrier

Supported by the General Program of National Natural Science Foundation of China (81271307).

✉ Xinyue Qin
qinxinyue01@163.com

[1] Department of Neurology, The First Affiliated Hospital of Chongqing Medical University, No. 1 You Yi Road, Chongqing 400016, People's Republic of China

[2] Department of Medicine, Drexel University College of Medicine, Philadelphia, PA 19129, USA

Introduction

Ischemic stroke and ischemia–reperfusion (I/R) injury can lead to the damage of the blood–brain barrier (BBB) and result in brain vasogenic edema [1, 2]. The process include oxidative stress, inflammation, apoptosis, excitotoxicity, and intracellular calcium overload. The BBB impedes influx of most compounds from the blood to brain, which is comprised of endothelial cells, pericytes, astrocytes, neurons, and the extracellular matrix, collectively known as the neurovascular unit [3]. Oxidative stress caused by post I/R can be broadly defined as excessive levels of reactive oxygen species (ROS), which impairs protein synthesis, causes deleterious DNA mutations, and ultimately results in brain cell apoptosis [4–6]. Considerable experiments indicate that ROS increases permeability of the BBB by activating matrix metalloproteinases (MMPs), degrading tight junction (TJ) proteins and impairing endothelial cells [7–10]. Therefore, protection of the BBB is one of the important targets of stroke treatment.

The focus of the research of stroke pathophysiology has recently shifted from conventional vascular concepts to the complex interplay of molecular mechanisms involving the neurovascular unit [11]. Specifically, extracellular matrix (ECM) proteins have been of interest. Fibulin-5 is a 66-kD glycoprotein secreted by various vascular cells, including

Published online: 30 May 2015

vascular smooth muscle cells (SMCs), fibroblasts, and endothelial cells [12, 13]. Fibulin-5 has been widely studied in tumor growth and invasion due to its inhibitory effect on the angiogenesis, proliferation, and migration of tumor cells [14–17]. The upregulation of fibulin-5 has been observed in vascular injury, such as atherosclerotic plaques and neointimal balloon injury, as well as in vascular endothelial cells induced by hypoxic stress [18–21]. Marie K. Schluterman et al. (2010) has reported that fibulin-5 prevents ROS production by blocking the interaction between fibronectin and β1 integrins [22], while fibronectin-α5β1 integrin is strongly upregulated in the vessels of the CNS ischemic penumbra [23, 24]. In addition, fibulin-5 has been identified as a novel binding protein for extracellular superoxide dismutase (ecSOD) to promote $O_2\cdot^-$ scavenging in the vascular extracellular space and to regulate the vascular redox state [25]. Therefore, we hypothesize that overexpression of fibulin-5 may help reduce production of ROS following cerebral ischemia and may thereby be neuroprotective.

In this study, we detected the effects of overexpressed fibulin-5 on blood–brain barrier and brain edema after ischemia/reperfusion injury in middle cerebral artery occlusion (MCAO) rats.

Materials and Methods

Animals and Groups

Ninety-five male Sprague-Dawley rats weighing 200 to 250 g were randomly divided into five groups to determine the optimal viral titer for the adenovirus experiments. Animals were divided into NS control (n=19), empty carrier recombinant adenovirus (Ad-HK) (n=19), low titer fibulin-5 overexpression recombinant adenovirus (Ad-FBLN) (n=19), medium titer Ad-FBLN (n=19), and high titer Ad-FBLN groups (n=19). All samples in this section were collected at 3 or 7 days after injection.

Male Sprague-Dawley rats weighing 200 to 250 g were randomly assigned into four groups: sham (n=50), ischemia/reperfusion (I/R) (1 day (1d), n=50; 3 days (3d), n=37), Ad-FBLN treatment (1d, n=50; 3d, n=37), or Ad-HK (1d, n=50; 3d, n=37). All samples and variables in this study were collected at 1 or 3 days after reperfusion. All protocols for animal experiments were approved by the Administrative Panel on Laboratory Animal Care of Chongqing Medical University.

Recombinant Adenovirus

Fibulin-5 overexpression recombinant adenovirus (Ad-FBLN) and empty carrier recombinant adenovirus (Ad-HK) were purchased from the Shanghai Neuron Biotech Co., Ltd. The virus was amplified in human embryo kidney 293 (HEK293) cells and purified by Sartorious Vivapure Adeno PACK 20. The 50 % tissue culture infectious dose (TCID50) method was applied to detect viral titer [26].

Stereotactic Surgery

We chose three different titers of Ad-FBLN and Ad-HK to stereotactically inject into the right cortex of rats. The injected rats underwent dextral MCAO/reperfusion 7 days post-injection. The bregma was selected as stereotaxic zero and injections performed at 1.0 mm rostral to the bregma and 2.0 mm lateral to the midline, 1.2 mm ventral to the dura and 3.0 mm caudal to the bregma, and 1.5 mm lateral to the midline and 1.2 mm ventral to the dura [27]. A total volume of 2 μl was injected at a rate of 0.2 μl/min at each microinjection site, and the microinjector was kept immobile for 5 min before withdrawal.

Middle Cerebral Artery Occlusion/Reperfusion Model

Right cerebral middle artery occlusion was induced by intraluminal suture. MCAO model with 90 min of ischemia was followed by reperfusion as described in a previous report [28]. Briefly, rats were anesthetized with 3.5 % chloral hydrate (350 mg/kg). Right external carotid artery (ECA), internal carotid artery (ECA), and common carotid artery (ECA) were exposed through a midline neck incision with careful conservation of the vagus nerve. ECA was coagulated, and a nylon filament suture coated with paraffin wax at the head end was introduced into ICA through the ECA stump. The suture was advanced about 18 mm from the carotid bifurcation until mild resistance was felt. After 90 min of occlusion, the rats were re-anesthetized and the filament was withdrawn from ICA to induce reperfusion. Animals in the sham group were treated similarly, except that the filament was not advanced to the origin of the MCA. Body temperature was maintained at 37 ±0.5 °C with heating pads until recovery from surgery. Rats without neurological deficit or that suffered subarachnoid hemorrhage after reperfusion were excluded from the present study. Physiological parameters were monitored during the whole process. A laser Doppler flow (LDF; Periflux system 5000; Perimed) was used to measure regional cerebral blood flow (rCBF) during surgery to confirm the successful occlusion of MCA.

Detection of Virus Delivery

Virus delivery was determined through observing green fluorescent protein (GFP) under the microscope [29]. Transfection efficiency was defined as the ratio of GFP-positive cells to total cells. To determine the most optimal therapeutic viral titer, RT-PCR and western-blotting were used to verify the level of fibulin-5

expression after transfection. Inflammation around the injection sites was examined by ELISA kit of IL-1β.

MRI Examination

Edema of post-ischemia brain was examined in a 1.5-Tesla (T) MRI animal scanner (Magnetom Trio with TIM system, Siemens, Erlangen, Germany). At 1 and 3 days after reperfusion, the rats in each group underwent MRI by placing it in a custom-made "birdcage coil" (inner diameter of 30 mm) for signal excitation and detection. MRI parameters were set at TE=92 ms, TR=3620 ms, FOV=8×8 cm, M=256×256, NA=2, thickness=2 mm, and gap=0 mm. After the optimal adjustment of contrast, hemisphere intensity was examined by Image J 1.42q software (National Institutes of Health, Bethesda, MD, USA) by measuring the "mean gray value." Similar to a previous report [30], the intensity percentage of the ipsilateral hemisphere against the contralateral hemisphere was calculated and then statistically analyzed.

Evans Blue Leakage

According to the previous description [31], Evans blue dye (Sigma-Aldrich, St. Louis, MO, USA, 4 %, 3 ml/kg) in 0.9 % saline was injected into the tail vein. Two hours after injection, rats were anesthetized with 3.5 % chloral hydrate (350 mg/kg) and transcardially perfused with 200–250 ml physiological saline. Then, brains were removed and each hemisphere was weighed. The samples were cut up and soaked in formamide (1 ml/100 mg) at 60 °C for 24 h. Before measuring the optical density (OD) values, the samples were centrifuged at 5000×*g* for 20 min, and then the supernatant was centrifuged at 10, 000×*g* for 10 min at 4 °C. The fluorescence of extracted dye was determined at 620 nm.

Infarct Volume and Neurological Scores

2,3,5-Triphenyltetrazoliumchloride (TTC) staining is the classic method used to measure infarct volume [32]. Coronal sections of brain were obtained via a brain slicer (Activational Systems, Warren, MI, USA) in 2-mm spacing. Slices were then immersed in 2 % TTC at 37 °C in the dark for 30 min and photographed. The infarct size was measured according to the method described by Kawamata and colleague [33].

Neurological scores were used to evaluate deficit after surgery as previously described [34]. The scoring system was defined as follows: 0=no deficit, 1=flexion of contralateral torso and forelimb upon lifting of the whole animal by the tail, 2=circling to the contralateral side when held by tail with feet on floor, 3=spontaneous circling to contralateral side, and 4=no spontaneous motor activity. Scoring of each rat was performed within 1 min and repeated three times. Any score higher than 0 was considered a behavioral deficit.

Immunofluorescence Staining and Confocal Microscopy

Coronal fresh frozen sections with 10-μm thickness were chosen on which to perform immunofluorescence staining. When slices were completely air-dried, they were treated with 0.01 mol/l sodium citrate buffer (pH 6.0) in a microwave oven for 20 min at 95 °C for antigen retrieval and then washed with phosphate-buffered saline (PBS) three times. After that, the slices were treated with 10 % normal donkey serum to block non-specific binding sites at 37 °C for 30 min. Slices were then incubated with primary antibodies including occludin (1:25, Invitrogen, USA) and RECA-1 (1:100, AbD Serotec, UK), which were diluted in PBS and kept overnight at 4 °C. After rewarming at room temperature and washing with PBS, the slices were incubated at 37 °C for 90 min with secondary antibodies, including Goat anti-Rabbit IgG (H+L) Secondary Antibody, Alexa Fluor® 350 conjugate (1:200, Thermo Fisher Scientific Inc., USA), and Goat anti-Mouse IgG (H+L) Secondary Antibody, Alexa Fluor® 647 conjugate(1:100, Thermo Fisher Scientific Inc., USA). The coverslipped slices were analyzed and photographed under a laser scanning confocal microscope (A1R, Nikon, Japan; TCS SP2, Leica, Germany).

Quantitative Real-Time PCR

RNA samples were extracted from brain tissue using Trizol reagent (Takara, Japan). According to the manufacturer's instructions, the procedures were as follows: frozen tissue was homogenized in RNAiso plus and then chloroform was added at one fifth of total volume. After centrifuging, the supernatant was transferred into isopropyl alcohol to precipitate RNA. The samples were then washed with 75 % ethanol and dissolved in RNAase free water. The concentration and purity of RNA were determined at 260/280 nm. Reverse transcriptase kit (Takara, Japan) was used to reverse transcribe total RNA into cDNA. Real-time fluorescent detection PCR (RT-PCR) analysis was performed with Thermal Cycler Dice Real Time System (Thermo, USA) and the SYBR PrimeScript PCR kit (Takara, Japan). Quantitative RT-PCR (qPCR) was performed via a Bio-Rad CFX96 instrument (Bio-Rad, USA). The following PCR protocol was used: 30 s at 95 °C, followed by 40 cycles of denaturation at 95 °C for 5 s, and annealing plus extension at 60 °C for 30 s. The level of fibulin-5 messenger RNA (mRNA) was normalized to β-actin. The primers were as follows: fibulin-5 forward primer 5′-GCCCTACTCCAA TCCCTACTCT-3′, reverse primer 5′-TACCCTCCTTCC GTGTTGATAC-3′; and actin forward primer 5′-CACCCG CGAGTACAACCTTC-3′, reverse primer 5′-CCCATACC CACCATCACACC-3′. The results were expressed as fold induction relative to controls.

Western Blot

The isolated ischemic cerebral cortex was homogenized in ice-cold lysis buffer containing 1 ml Radio Immunoprecipitation Assay Lysis Buffer and 5 μl of 100 μg/ml Phenylmethyl Sulphonyl Fluoride (Beyotime, China), 5 μl phosphatase inhibitor, and 1 μl proteinase inhibitor mixture for purifying proteins according to the manufacturers' instructions. Protein concentration was determined using the bicinchoninic acid (BCA) method (Pierce, Rockford, IL). Equal amounts of protein per lane (50 μg) were loaded onto an 10 % polyacrylamide gel and separated by electrophoresis at 80 V for 90 min. Proteins were then transferred to a PVDF membrane (Millipore, USA) at 250 mA for 70 min and the membrane was blocked with 5 % nonfat dried milk/0.05 % Tween 20 in Tris-buffered saline. The membrane was then incubated overnight at 4 °C with primary antibodies: anti-fibulin-5 (1:900, Millipore, USA), anti-occludin (1:200, Invitrogen, USA), anti-MMP-9 (1:200, Santa Cruz, CA, USA), anti-p-Akt (1:1000, Cell Signaling Technology, USA), and anti-caspase-3 (1:1000, Abcam, USA). Following washing, the membranes were incubated with peroxidase conjugated rabbit anti-goat IgG or anti-mouse IgG in blocking solution for 1 h at 37 °C. The Western blot results were quantified by densitometry. Relative optical density of protein bands was measured following subtraction of the background.

Ultrastructure Examination

Transmission electron microscopy was used to detect BBB ultrastructure. At 24 h after 2 % glutaraldehyde in 0.1 mol/l phosphate buffer reperfusion, approximately 1 mm^3 of ischemia penumbra cortex was taken and fixed in fresh prepared 3 % glutaraldehyde overnight at 4 °C. The tissue was washed with 0.1 mol/l phosphate buffer three times and then was post-fixed in 1 % osmium tetroxide for 2 h at 4 °C. Grade acetone and Epon 812 were used to dehydrate and embed samples. The ultrathin sections of cortex were stained with uranyl acetate and lead citrate. All specimens were processed as above procedures and then examined under a scanning electron microscope (JSM-5600LV, JEOL, Tokyo, Japan).

TUNEL Staining

Paraffin brain sections were prepared to perform TUNEL staining to examine nuclear DNA fragmentation according to the manufacturer's instructions (Roche Applied Science, Indianapolis, IN). Stained sections were imaged by fluorescent microscopy under a Leica DM5000B microscope and LEI-750 camera (Leica Microsystems, Germany). Hoechst dye and a cube were used to stain and visualize all nuclei (blue). CD31 were used to stain vessels (red). Dead cells were labeled visible green using the L5 cube. The additional sections on TUNEL staining were continued with AP converter (Roche Applied Science, Indianapolis, IN) and BM purple AP substrate (Roche Applied Science, Indianapolis, IN). Confocal fluorescence microscope (TCS SP8, Leica, Germany) was used for brightfield detection of stained sections [35].

ELISA

Brains were collected at 1 and 3 days after ischemia reperfusion and kept at −80 °C for measuring ROS generation with a rat ROS-horseradish peroxidase (HRP) conjugate ELISA kit (Cusabio, Inc.) according to the manufacturer's instructions [36]. A standard curve was constructed from the standards provided by the manufacturers. Antibody specific for ROS was pre-coated onto a microplate. After washing, avidin-conjugated HRP was incubated with the supernatant of the samples. Then, a substrate solution was added to the wells for color development. Finally, the optical density of each well was measured using a microplate reader (Mss, Thermo, USA) at 450 nm.

Transfected brains in different adenovirus titer at 7 days after injection were similarly prepared for measuring IL-1β level with an ELISA kit (Neobioscience Technology Company, Shanghai) according to the manufacturer's protocol.

Rac1 Assay

Rac activation assays were performed using Rac Activation Assay Biochem kit (BK035, Cytoskeleton, Denver, CO). Magnesium-containing lysis buffer was used to wash precipitated complexes three times, and the complexes were boiled in sample buffer. SDS-PAGE was used to fractionate proteins, which were then subjected to western blot analysis using the anti-Rac1-specific antibody supplied by the kit [37].

Determination of SOD

The level of SOD in all groups was measured 1 and 3 days after ischemia reperfusion using a kit (Nanjing JianCheng Biological Engineering Institute, Nanjing) following the manufacturer's protocols. After the reaction, the optical density (OD) of samples was measured at 550 nm for SOD activity in a microplate reader (Mss, Thermo, USA). SOD was calculated with the formula provided in the manufacturer's instructions.

Statistical Analysis

SPSS 16.0 for windows was used to perform statistical analyses. All results were presented as means±standard deviation (SD). Statistical differences between the control and each group of ischemia were analyzed using one-way analysis of

variance (ANOVA) followed by post hoc Tukey tests. P value <0.05 was considered statistically significant.

Results

Titers, Delivery Efficacy, and Toxicity of Recombinant Adenovirus

The three titers of Ad-FBLN used were 4.75×10^{10} pfu/ml (low titer), 9.5×10^{10} pfu/ml (medium titer), and 1.9×10^{11} pfu/ml (high titer). The titer of Ad-HK used was 4.0×10^{10} pfu/ml. GFP-positive cells were observed in the cortex as well as lateral ventricle and choroid plexus 7 days after injection of all three titers of Ad-FBLN and Ad-HK (Fig. 1a). The transfection efficiency of medium titer injection (60.12±10.34 %) and high titer injections (62.51±9.71 %) were similar (P>0.05) as determined by GFP expression relative to total cell expression, and both were better than that of the low titer group (20.54±4.35 %, P<0.01).

The mRNA and protein expression of fibulin-5 were used to further confirm transfection efficiency at 7 days after injection. The expression of mRNA and protein in all three titers of Ad-FBLN groups was higher than that of the Ad-HK group (P<0.05). Expression in the medium and high titer groups was significantly higher than the low titer group (P<0.05, Fig. 1b, c).

The inflammatory response after adenovirus injection was estimated with IL-1β with an ELISA kit (Fig. 1d). The level of IL-1β increased at 3 days after injection in the high titer group (62.60±12.36 pg/mg), medium titer group (34.21±3.70 pg/mg), low titer group (33.86±4.70 pg/mg), and Ad-HK group (32.17±4.30 pg/mg) as compared to the NS control group (19.17±2.80, P<0.01). IL-1β in the high titer group (121.00±23.77 pg/mg) was significantly increased at 7 days after injection compared to the NS control group (23.18±2.70 pg/mg, P<0.01), Ad-HK group (35.30±3.80 pg/mg, P<0.01), low titer group (33.40±6.20 pg/mg, P<0.01), and medium titer group (35.17±5.20 pg/mg, P<0.01). There was no statistically significant difference of IL-1β between the Ad-HK, low titer, and medium titer groups. Therefore, the medium titer (9.5×10^{10} pfu/ml) dose was chosen as the most optimal one for treatment. The titer of Ad-HK was increased to 1.7×1011 pfu/ml through CsCl gradient centrifugation(30,000 rpm, 4 °C,16 h) and then regulated to the medium titer (9.5×1010 pfu/ml).

Overexpression of Fibulin-5 Showed no Effect on Infarction Volume but Improved Neurological Deficits

Infarct volume was detected by TTC staining 1 day after MCAO. Normal brain tissue was stained red, while the infarct lesion remained white (unstained) (Fig. 2a). Brain infarct size was significantly increased in I/R 1d (0.32±0.07), I/R+Ad-FBLN (0.32±0.07), and I/R+Ad-HK (0.31±0.04) groups when compared with the sham group (P<0.01). However, no significant differences were found between I/R 1d, I/R+Ad-FBLN, and I/R+Ad-HK groups (P>0.05, Fig. 2b). Therefore, the intervention did not reduce infarct volume.

Neurological score was conducted to evaluate neurological behavior impairment in the different groups (Fig. 2c). Rats in I/R 1d and I/R 3d groups exhibited severe neurological deficits as compared to the sham group (6.00±0.41 vs 14.63±0.48 or 7.50±1.47 vs 14.50±0.58, P<0.01). In the I/R 1d+Ad-HK (5.75±0.65) and I/R 3d+Ad-HK (7.75±1.32) groups, the neurological deficits were not significantly different from the I/R 1d and I/R 3d groups (P>0.05). However, overexpression of fibulin-5 prevented neurological impairment after I/R 1d (10.50±0.41, P<0.01) and 3d (11.50±1.29, P<0.05).

Overexpression of Fibulin-5 Attenuated Apoptosis Following I/R

TUNEL staining was used to determine if overexpression fibulin-5 prevented tissue cells from undergoing transient ischemia-induced apoptosis (Fig. 3). A few apoptotic cells were scattered in the cortex in the sham group, while there were many TUNEL-positive cells in I/R and I/R+Ad-HK groups. Intervention with Ad-FBLN reduced the number of positively stained cells, suggesting that fibulin-5 overexpression attenuated cortical cell apoptosis. In addition, Ad-FBLN greatly decreased the apoptosis of endothelial cells after I/R compared with I/R and I/R+Ad-HK groups.

To further detect differences in apoptosis among all groups at 1 day following I/R, apoptosis-related proteins (Caspase-3 and p-Akt) were measured with Western blot. Increased cleaved caspase-3 protein expression was observed in I/R and I/R+Ad-HK groups as compared to the I/R+Ad-FBLN group (Fig. 4a). Decreased p-Akt protein expression was also observed in I/R and I/R+Ad-HK groups as compared to the I/R+Ad-FBLN group (Fig. 4b).

Overexpression of Fibulin-5 Decreased Post-stroke Edema and Reduced Evans Blue Extravasation

To examine brain edema induced by I/R, we performed T2-weighted MRI. Rats in all groups were evaluated for cerebral edema (Fig. 5a). No edema was detected in the sham group at both examined time points. In contrast, edema was found in the I/R 1d group (170.39±21.54) versus I/R 1d+Ad-HK(170.66±21.88) and in the I/R 3d (163.99±14.33) versus I/R 3d+Ad-HK group(159.79±20.27) without significant differences (P>0.05). However, with overexpression of fibulin-5, the cerebral edematous area was significantly reduced at 1d (117.61±25.05) and 3d (118.43±13.57) (P<0.05). Quantitative analysis of MRI was conducted based on intensity analysis of the images (Fig. 5b).

The amount of Evans blue dye extravasation in the I/R 1d (6.87±0.69) and I/R 3d (5.79±0.77) groups was distinctly increased compared to the sham group (1.62±0.55 and 1.35

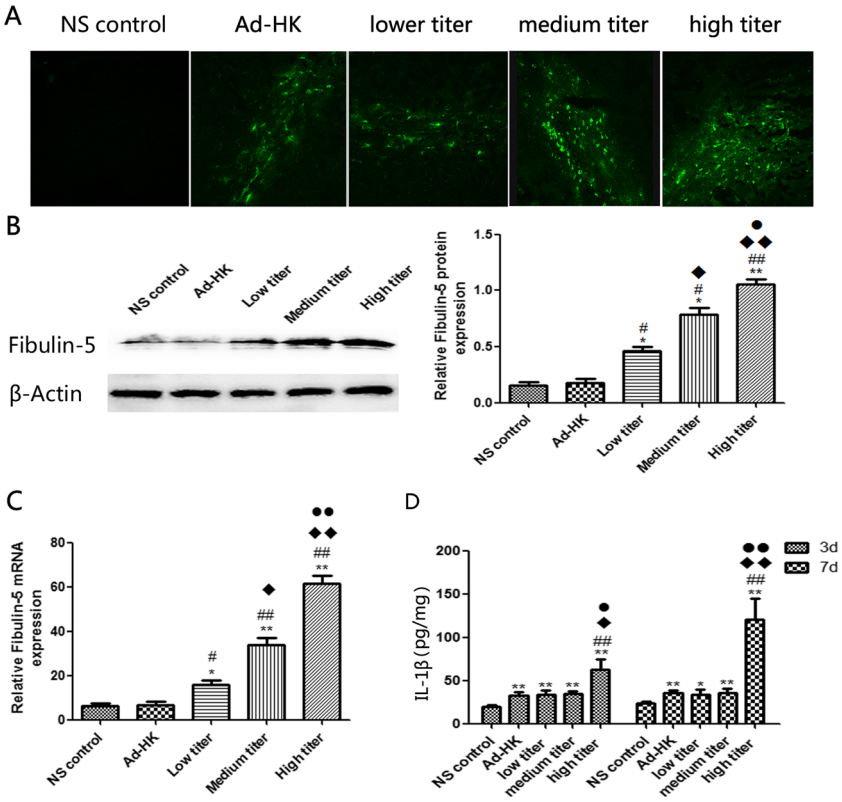

Fig. 1 Adenovirus delivery in peri-infarct cortex 7 days after injection. **a** GFP-positive cells are observed in NS, Ad-HK, and three different titers of Ad-FBLN groups (×200). A few GFP-positive cells are localized in the ischemic cortex and observed with medium (9.5×10^{10} pfu/ml) and high titer (1.9×10^{11} pfu/ml) groups. *Scale bars*: 150 μm. **b** mRNA expression of fibulin-5 mRNA in the cortex is increased with all three titers of Ad-FBLN. **c** Fibulin-5 protein is increased in the cortex of all three Ad-FBLN groups. *Bars* represent the relative density of fibulin-5 to β-actin in the cortex. *$P<0.05$, **$P<0.01$ versus NS group, $^{\#}P<0.05$, $^{\#\#}P<0.01$ versus Ad-HK group, ♦$P<0.05$, ♦♦$P<0.01$ versus low titer group, ●$P<0.05$, ●●$P<0.01$ versus medium titer group

±0.55, $P<0.01$) (Fig. 6a, b). Similarly, the I/R 1d+Ad-HK (7.39±1.05) and I/R 3d+Ad-HK (5.87±1.10) groups had increased Evans blue dye extravasation compared to the sham group($P<0.01$). There was no difference between the I/R 1d, I/R 1d+Ad-HK, I/R 3d, and I/R 3d+Ad-HK groups($P>0.05$)(-Fig. 6a, b). In contrast, intervention of Ad-FBLN significantly decreased the extravasation of Evans blue dye in the I/R 1d+Ad-FBLN (3.79±0.93, $P<0.01$) and I/R 3d+Ad-FBLN (3.34 ±0.85, $P<0.05$) groups.

Collectively, these data demonstrate that overexpression of fibulin-5 attenuated BBB permeability induced by I/R.

Effect of Overexpression of Fibulin-5 on Ultrastructure Alterations of BBB

BBB ultrastructure was examined. As shown in Fig. 7, the basement membrane and the tight junctions of the BBB were disrupted in all I/R and I/R+Ad-HK groups, and greater continuous basement membrane and tight junctions were observed in I/R+Ad-FBLN groups, indicating higher BBB integrity.

Overexpression of Fibulin-5 Suppressed Expression of MMP-9 and Reversed the Reduction of Occludin Degradation

Confocal microscopy revealed that occludin, a tight junction protein, localized between endothelial cells as continuous lines in sham group. These continuous distributions were disrupted in all I/R groups and became intermittent lines, as well as becoming unstained, which suggests degradation of occludin induced by I/R. Ad-FBLN treatment attenuated occludin degradation (Fig. 8a). Results were confirmed by Western blot (Fig. 8b, e).

In order to gain insight into the role of overexpression of fibulin-5 in maintaining BBB integrity, MMP-9 expression was detected. As shown in Fig. 8b, d, it is upregulated in the I/R 1d and I/R 3d groups compared to sham ($P<0.01$). Meanwhile, no significant difference was found between I/R 1d and I/R 1d+Ad-HK($P>0.05$) or I/R 3d and I/R 3d+Ad-HK($P>0.05$). However, administration of Ad-FBLN significantly decreased the expression of MMP-9 compared to other control groups ($P<0.05$). These results suggest that overexpression of fibulin-5 attenuates BBB permeability after I/R by interfering with MMP-9 expression.

Overexpression of Fibulin-5 Reduced the Level of ROS by Inhibiting Expression of Activated Rac-1

Since it has been reported that fibulin-5 competes with fibronectin for β1 integrin binding to downregulate ROS production, we examined ROS levels. Groups receiving I/R had higher levels of ROS via ELISA as compared to sham (3.58 ±0.40 vs 1.55±0.39 or 2.84±0.24 vs 1.31±0.22, $P<0.01$). No difference was found between I/R and I/R+Ad-HK groups at 1 or 3 days following I/R ($P>0.05$). Consistent with previous

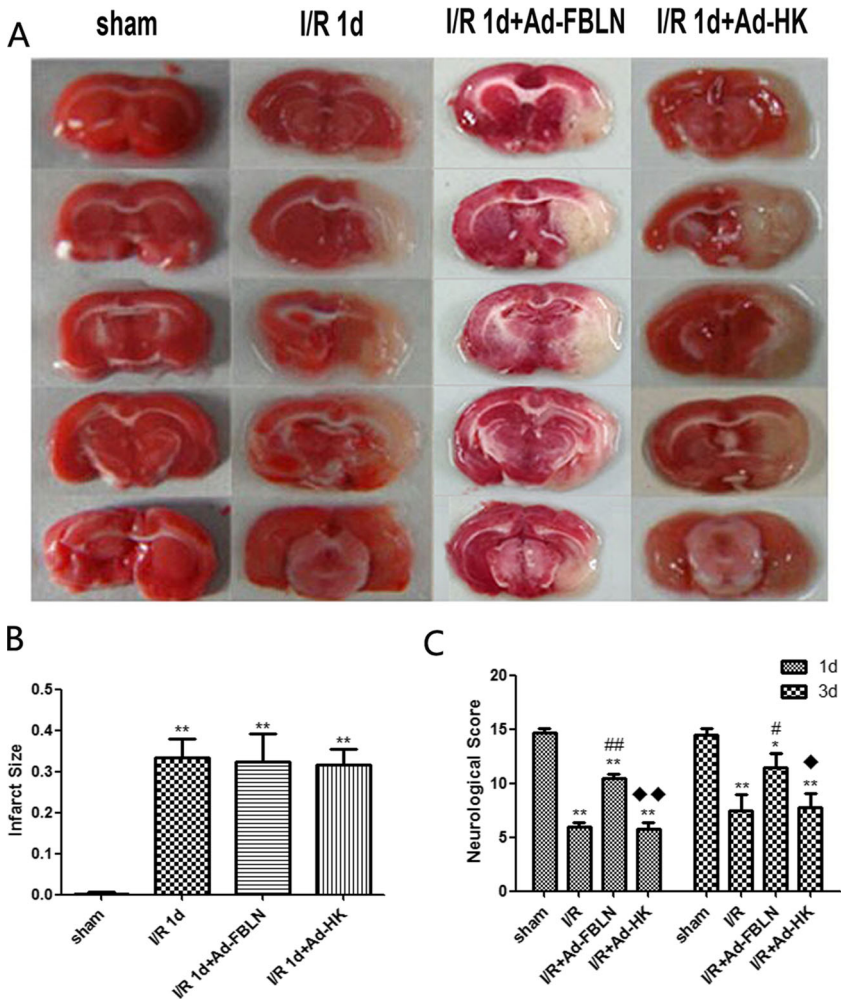

Fig. 2 Overexpression of fibulin-5 does not reduce brain injury but improves neurological outcome. **a** Photographs of rat brain TTC staining in the four groups. **b** Quantitative analysis of infarct size in four groups. **c** Neurological scores of animals in different groups. *$P<0.05$, **$P<0.01$ versus sham; $^{\#}P<0.05$, $^{\#\#}P<0.01$ versus I/R; ♦$P<0.05$, ♦♦$P<0.01$ versus I/R+Ad-FBLN

data, Ad-FBLN intervention significantly reduced the production of ROS at both examined time points as compared to non-treated groups (2.45±0.36 and 2.04±0.38, $P<0.01$ and $P<0.05$) (Fig. 9a).

To gain insight into the mechanism of ROS reduction by overexpression of fibulin-5, Rac-1 assay was performed to detect GTPase Rac-1 activation (Fig. 9c). Paola Chiarugi et al. reported that integrin-induced ROS production required functional Rac-1 [38]. Enhanced levels of GTP Rac-1 was detected in the I/R 1d group compared to the sham group($P<0.01$), and there were statistical significant differences between the I/R 1d+Ad-FBLN and I/R 1d groups($P<0.05$) (Fig. 9d). Similar results were observed in all groups at 3 days following reperfusion ($P<0.05$) (Fig. 9d). The total level of Rac-1 was unchanged at both time points examined following reperfusion.

Overexpression of Fibulin-5 Reduces the Level of ROS Without Influencing SOD Content

Total SOD content was analyzed to determine its role in the balance of oxidative stress (Fig. 9b). All I/R groups had increased SOD levels as compared to sham (39.21±13.63 vs 81.06±7.88 or 42.90±8.72 vs 77.56±10.76, $P<0.05$ and $P<0.01$). However, there was no significant difference between I/R 1d and I/R 1d+Ad-HK groups (37.54±13.70, $P>0.05$). Similar results were also observed in I/R 3d and I/R 3d+Ad-HK groups (37.95±13.72, $P>0.05$). Interestingly, overexpression of fibulin 5 did not significantly change SOD levels (44.04±13.70 or 42.31±13.89, $P>0.05$). It might indicate that total SOD was not involved in the fibulin-5-mediated ROS decreases.

Discussion

Fibulin-5 plays a key role in the physiological process of tissue development, remodeling, and reparation [20, 39–41]. It has a direct effect on the efficiency of the vasculature because it is required for maturation of elastic fibers and it supports the blood vessel wall [18]. Williamson and colleagues have showed that fibulin-5 favored endothelial cell attachment to the ECM to preserve an intact endothelial cell monolayer

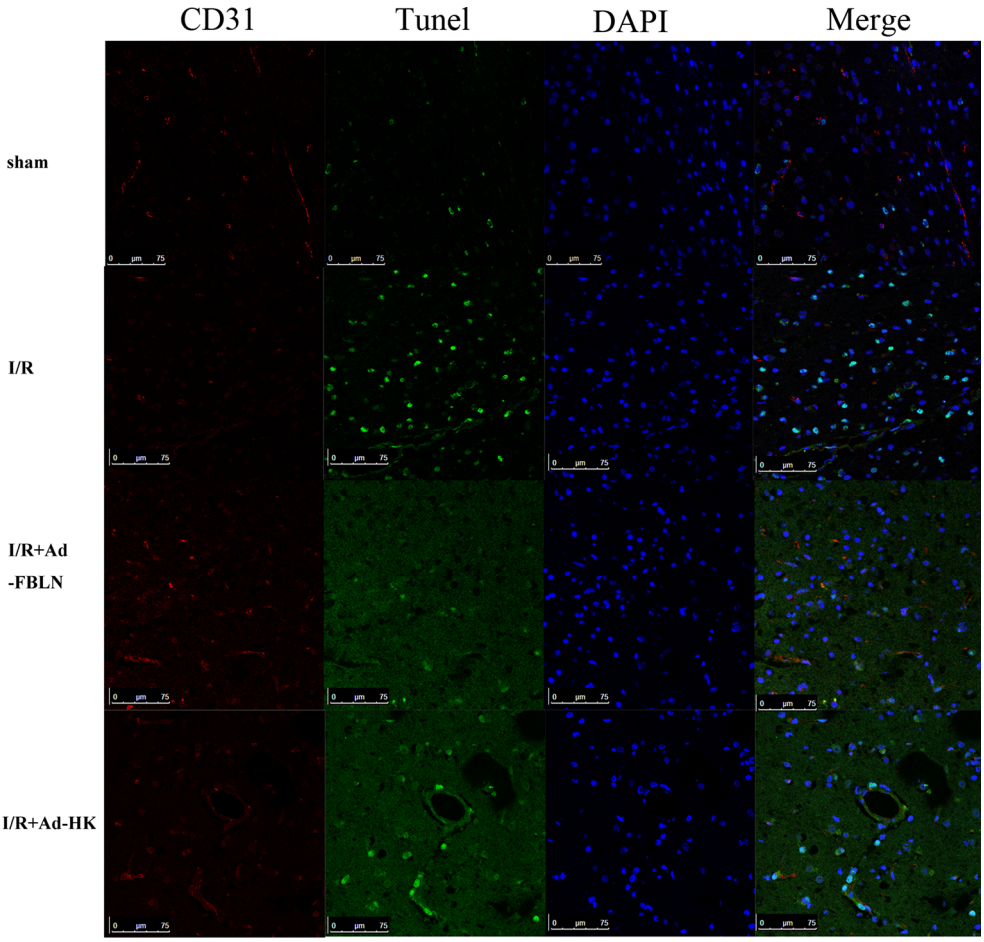

Fig. 3 Overexpression of fibulin-5 reduces brain cell apoptosis, especially vascular endothelial cells after I/R. The three-color labeled immunofluorescent staining of CD31 (*red*), 4,6-diamidino-2-phenylindole (DAPI) (*blue*), and nuclear DNA fragmentation of apoptotic cells (*green*) was used to detect the dead vascular endothelial cells and nuclei. *Scale bar*=25 μm (Color figure online)

structure and its functional characteristics [12]. Upregulation of fibulin-5 induced by hypoxic stress is considered an adaptive survival response of vessel endothelial cells [19]. In addition, a previous study has demonstrated that the interactions of the endothelial cell–matrix via the adhesion receptor β1-integrins (vertical adhesion) can directly affect TJ

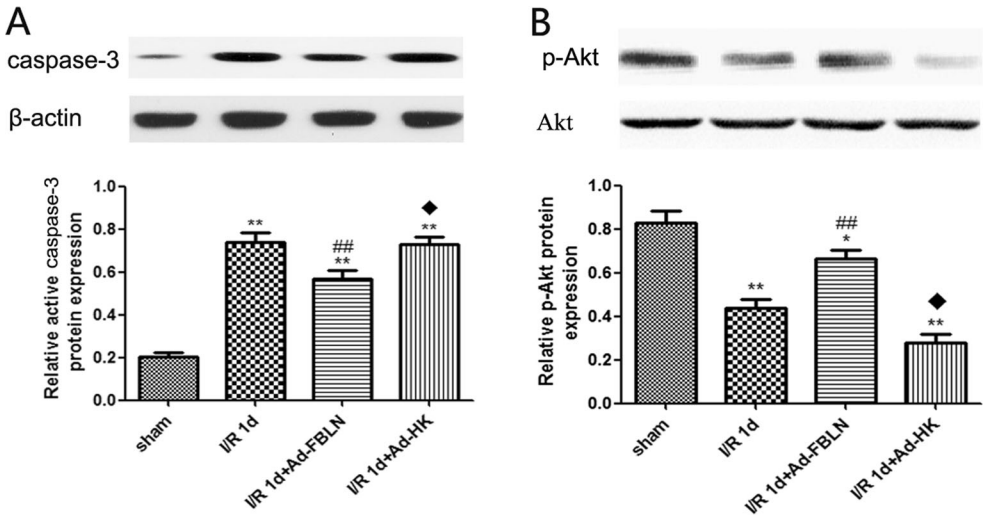

Fig. 4 Overexpression of fibulin-5 rescues the expression of caspase-3 and p-Akt in the cortex induced by ischemia. **a** Western blot analysis shows the expression of caspase-3 in the cortex. *Bars* represent the relative density of caspase-3 to β-actin. $^{**}P<0.01$ versus sham group; $^{\#\#}P<0.01$ versus I/R group; $\blacklozenge P<0.05$ versus I/R+Ad-FBLN group. **b** Western blot analysis shows the expression of p-Akt in the cortex. *Bars* represent the relative density of p-Akt to Akt. $^{*}P<0.05$, $^{**}P<0.01$ versus sham group; $^{\#\#}P<0.01$ versus I/R group; $\blacklozenge P<0.05$ versus I/R+Ad-FBLN group

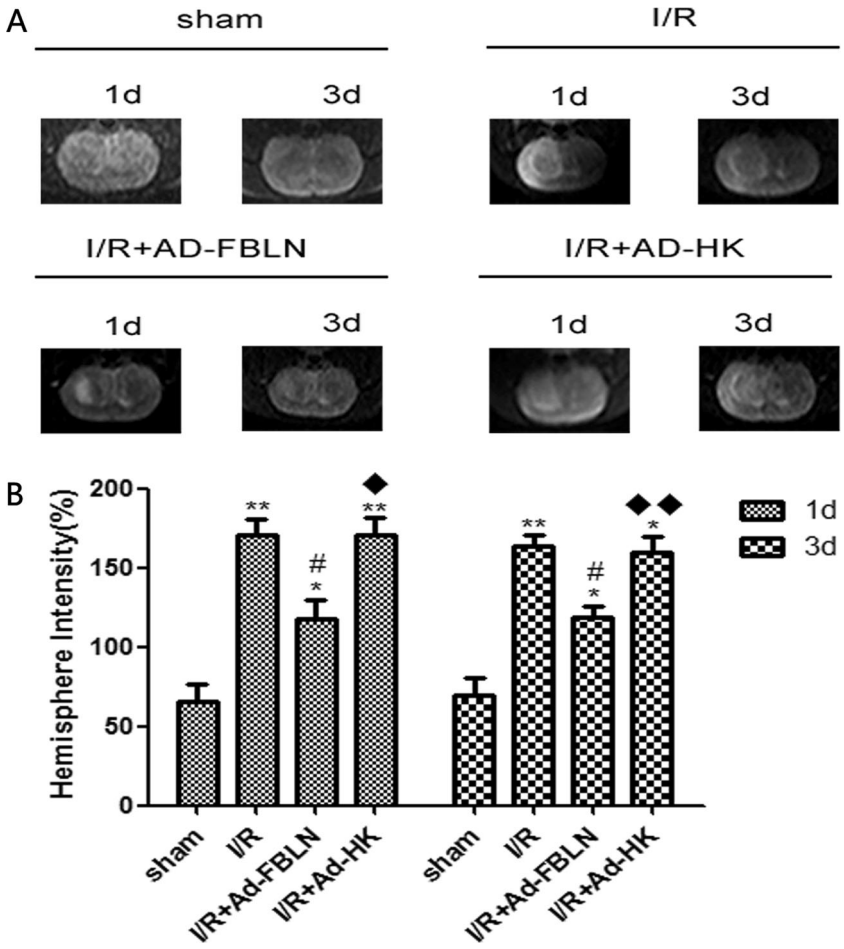

Fig. 5 T2-weighted MRI images of rat brains. **a** Representative MRI from rats in groups examined 1 day (1d) and 3 days (3d) after reperfusion, respectively. **b** Quantitative analysis of the MRI signal intensity in groups examined 1 and 3d after reperfusion, respectively. Ordinate: percentage of MRI intensity in ipsilateral hemisphere versus the contralateral hemisphere. *$P<0.05$, **$P<0.01$ versus sham group; $^{\#}P<0.05$ versus I/R group; ♦$P<0.05$, ♦♦$P<0.01$ versus I/R+ Ad-FBLN group

expression and inter-endothelial cell attachments (horizontal cohesion), thereby altering brain microvascular permeability [42]. Therefore, we chose the rat cerebral focal ischemia reperfusion model with overexpressing fibulin-5 to examine this effect in vessel endothelial cells and BBB structure.

Recombinant adenoviral vector has been used for intervention in CNS injury due to its safety and stability [43–45]. Given the side effects caused by an immune response to the recombinant adenovirus and its gene products, the early inflammatory response marker IL-1β was evaluated by ELISA around the injection site. Thus, both transfection efficiency and inflammation are typically taken into account to determine the best titer for intervention. Similar to previous research results, the medium titer group (9.5×10^{10} pfu/ml) was determined to be the optimal titer for intervention in the present study.

In the present study, overexpression of fibulin-5 did not show a significant change in the cerebral infarct volume after I/R at 1 day, even though it significantly decreased expression of Akt and caspase-3. This is the first report showing a protective effect of fibulin-5 on neurovascular endothelium. We further found that ROS production in the Ad-FBLN group was significantly reduced after I/R. In addition, there was a significantly increased level of activated Rac-1 (GTPase Rac-1) at 1 day after reperfusion, but the level was lower in the Ad-FBLN group as compared to the I/R and I/R+As-HK groups. These results are consistent with previous reports, which show a rapid and significant elevation of GTPase Rac-1 after cerebral ischemia reperfusion [37]. Therefore, we postulate that the anti-apoptotic effect of increased fibulin-5 can be achieved by the activation of Rac-1 and reduction ROS production.

Our data also show that overexpression of fibulin-5 improved post-stroke edema as detected by MRI examination. Evans blue extravasation was also reduced, suggesting a potential protective effect on the BBB. Massive brain edema induced by the leakage of BBB is the main cause of death in acute stroke [46]. Many reports show that brain edema is maximal 1–3 days after the onset of ischemia and then starts to decrease. We found fibulin-5 to be a promising intervention for decreasing post-stroke edema and protecting the BBB. BBB damage often involves increased expression of MMP-9 and the degradation of tight junction proteins. Our results show that expression of MMP-9 and degradation of occludin were suppressed by fibulin-5 overexpression. Similarly, lower levels of GTPase Rac-1 and ROS production were noted. Therefore, we postulate that increased fibulin-5 reduces

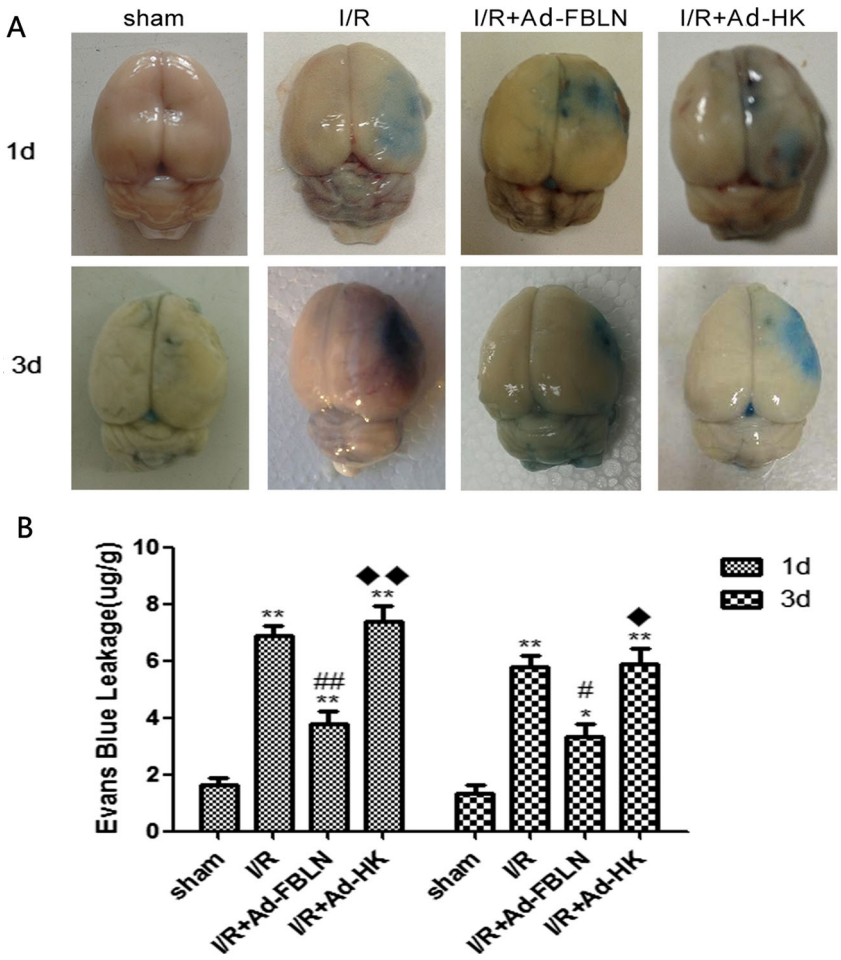

Fig. 6 Overexpression of fibulin-5 reduces Evans blue leakage in rats. **a** Representative images of brain Evans blue leakage in all groups. **b** Quantitative analysis of Evans blue leakage. *$P<0.05$, **$P<0.01$ versus sham group; $^{\#}P<0.05$, $^{\#\#}P<0.01$ versus I/R group; ♦$P<0.05$, ♦♦$P<0.01$ versus I/R+Ad-FBLN group

post-stroke edema and BBB damage under the control of ROS production after I/R. Collectively, our results support the notion that overexpression of fibulin-5 has no effect on infarct volume after I/R, but it does protect brain and vascular endothelial cells from apoptosis at the cellular level. It is therefore likely that decreased cerebral edema and BBB extravasation

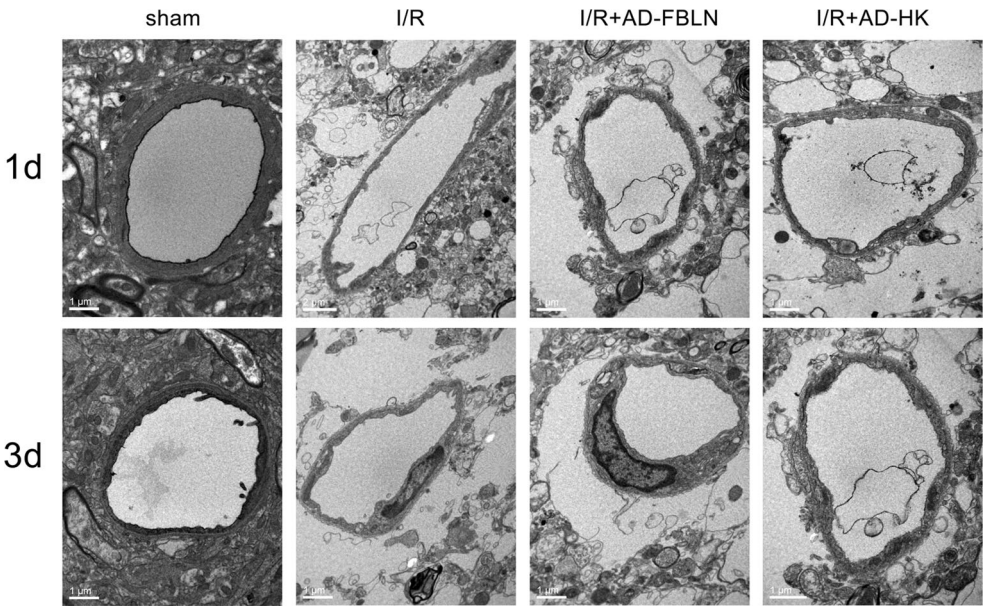

Fig. 7 Effect of increased fibulin-5 on blood–brain barrier ultrastructure in cortex. Normal basement membrane (*arrow*) and tight junctions (*arrowhead*) are visible in sham group. The basement membrane and tight junctions are disrupted in I/R and I/R+Ad-HK groups. More continuous basement membrane and tight junctions are observable in I/R+Ad-FBLN group. *Scale bar*=1 μm

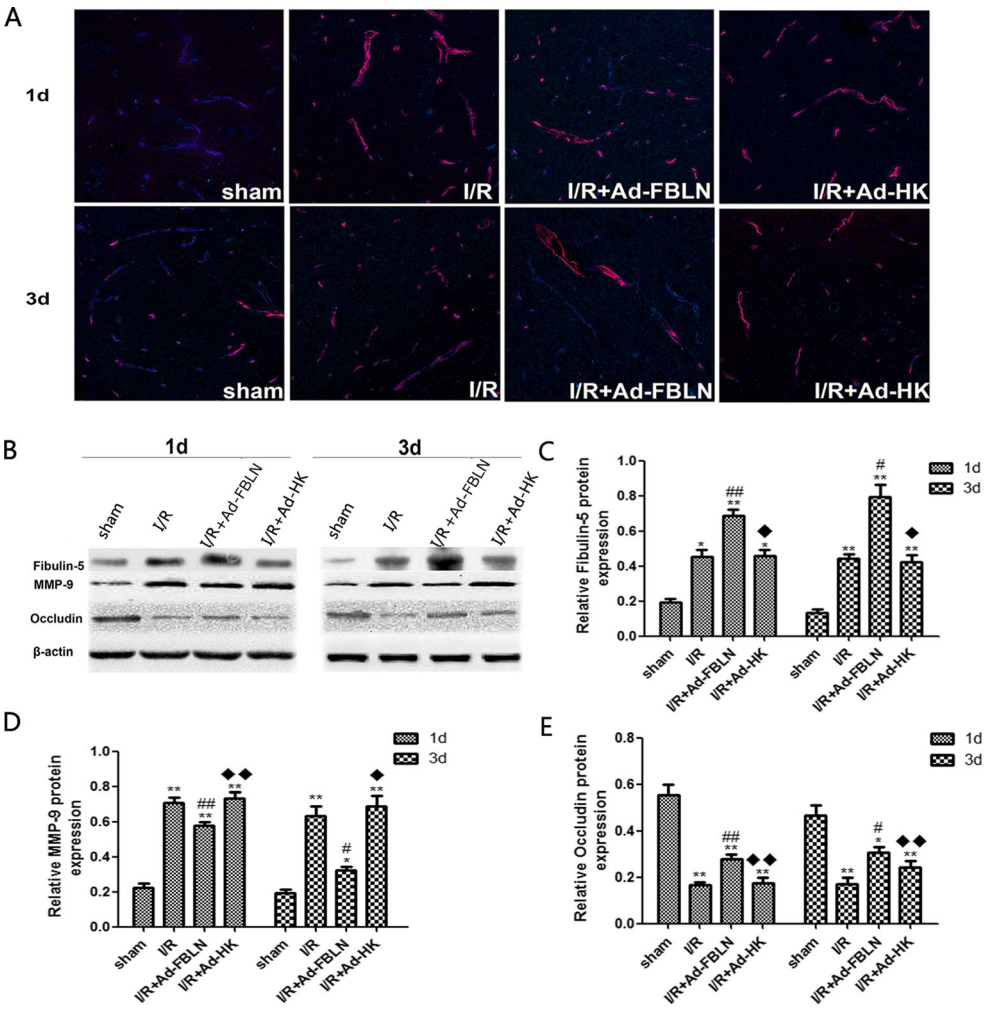

Fig. 8 Effect of increased fibulin-5 on MMP-9 and occludin expression. **a** Representative immunofluorescence confocal images of occludin. The distribution of occludin is localized at the periphery of endothelial cells with marker RECA-1 (*rose red*). The continuous distribution of occluding (*indigo*) in cortical microvessels is visible in sham group. The distribution of occludin is disrupted in I/R and I/R+Ad-HK groups. However, enhanced normal occludin staining is noticeable in the Ad-FBLN group. *Scale bars*=50 μm. **b** Western blot was used to detect the expression of fibulin-5, MMP-9, and occludin proteins at 1d and 3d after reperfusion. C.D.E. Western blot analysis shows the expression of fibulin-5, MMP-9, and occludin in the cortex, respectively. *Bars* represent the relative density of various proteins to β-actin. $*P<0.05$, $**P<0.01$ versus sham group; $^{\#}P<0.05$, $^{\#\#}P<0.01$ versus I/R group; $\blacklozenge P<0.05$, $\blacklozenge\blacklozenge P<0.01$ versus I/R+Ad-FBLN group (Color figure online)

are responsible for the neuroprotective effects of overexpressed fibulin-5.

Beyond the enhanced physical combination of endothelial cells and basement membrane assisted by fibulin-5, we also analyzed its unique ability to alter cell-ECM signaling and directly regulate proliferation, adhesion, and migration, which is achieved by its RGD-motif binding integrin such as αvβ3, αvβ5, and α5β1 [12, 14, 47–49]. It must be noted that fibulin-5 also regulates ROS production in endothelial cells and fibroblasts [22]. The α5β1 integrin serves as the primary fibronectin receptor. The binding of this integrin to fibronectin can stimulate downstream signaling, leading to ROS generation [8]. However, fibulin-5 competes with fibronectin for β1 integrin binding to prevent ROS production, since fibulin-5 functions as a blocking protein to control intracellular signaling without inducing integrin activation [8]. In the developing CNS, angiogenic capillaries express high levels of fibronectin and its receptor α5β1 integrin, and this expression is developmentally downregulated. On the other hand, fibronectin and its associated endothelial receptors α5β1 and αvβ3 integrins are strongly upregulated on angiogenic vessels in the ischemic penumbra following cerebral ischemia and the hypoxic CNS [23, 24]. Therefore, under the condition of cerebral ischemia reperfusion, the production of ROS will accordingly increase with the upregulated expression of fibronectin and integrin receptors. Increased expression of fibulin-5 following ischemia/reperfusion can be used as a promising mechanism to control ROS production.

GTPase Rac-1 modulates both LOX and NADPH oxidases, which are the sources of ROS [50]. At the same time, the small GTPase Rac-1 acts as the central component of the signaling machinery downstream of adhesion molecules [51, 52]. Integrin-induced ROS production requires Rac-1 activation [38]. Our experimental results are consistent with this mechanism. Under the intervention of overexpressed fibulin-5, the level of activated Rac-1 declined, suggesting that activated Rac-1 is involved in the fibulin-5-controlled integrin-induced ROS production following cerebral ischemia reperfusion. This finding helps elucidate the molecular mechanism of fibulin-5 in controlling ROS production.

The role of superoxide dismutase (SOD) enzymes is to prevent excessive ROS production. Cu/ZnSOD, MnSOD, and extracellular superoxide dismutase (ecSOD) are three

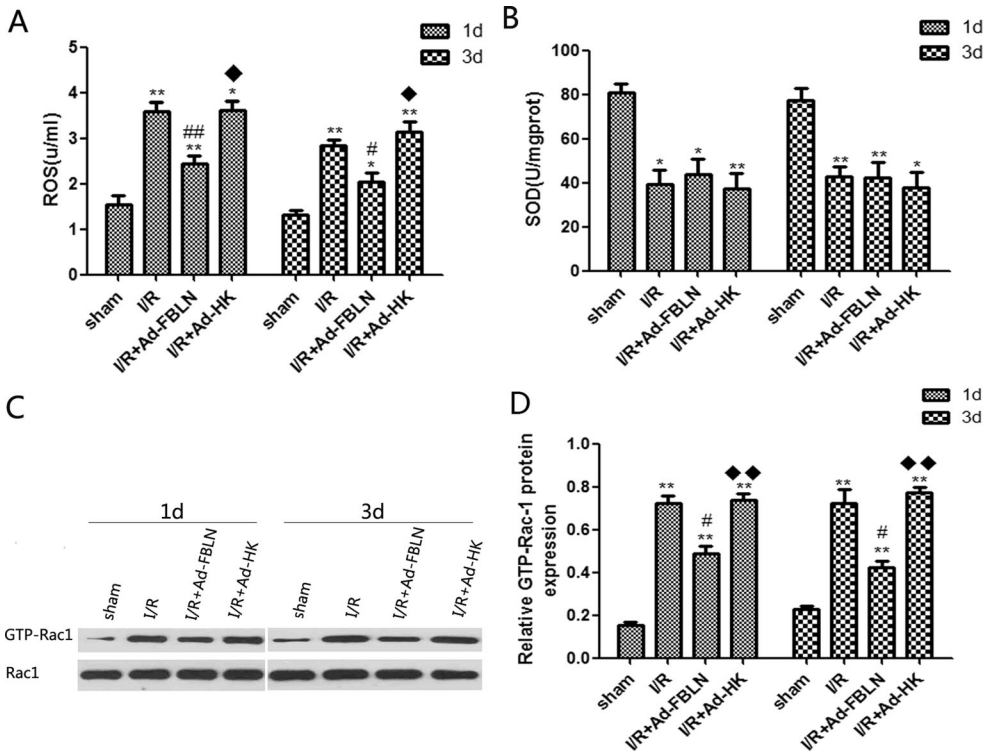

Fig. 9 Overexpression of fibulin-5 reduces ROS production by inhibiting the activation of Rac1 and does not affect SOD levels. **a** ROS production is significantly increased in I/R, I/R+Ad-FBLN, and I/R+Ad-HK groups as compared to sham group, and relatively reduced in I/R+Ad-FBLN group compared to I/R and I/R+Ad-HK groups. *$P<0.05$, **$P<0.01$ versus sham group; $^{\#}P<0.05$, $^{\#\#}P<0.01$ versus I/R group; ♦$P<0.05$ versus I/R+Ad-FBLN group. **b** SOD is significantly reduced in I/R, I/R+Ad-FBLN, and I/R+Ad-HK groups as compared to sham group. There are no significant difference between I/R, I/R+Ad-FBLN, and I/R+Ad-HK groups. *$P<0.05$, **$P<0.01$ versus sham group. **c** Rac1 activation is attenuated with fibulin-5 overexpression. **$P<0.01$ versus sham group; $^{\#}P<0.05$ versus I/R group; ♦♦$P<0.01$ versus I/R+Ad-FBLN group

isoforms of SOD that assist in the breakdown and clearance of ROS and their intermediates from tissues. The balance of oxidative stress should include two aspects: source and removal of the ROS. Our study assessed not only the source of ROS but also the SODs for ROS removal. The results showed that total SOD content in the treatment group had no significant difference compared to the other groups. It is possible that total SOD is not involved in the fibulin-5-mediated ROS production. Nguyen et al. has reported that fibulin-5 facilitates the localization of ecSOD to endothelial cells to modulate O_2 levels in the vasculature[25]. Levels of esSOD need to be analyzed to draw further conclusions.

The present study has demonstrated the novel notion that overexpression of fibulin-5 can reduce the generation of ROS in a cerebral ischemia reperfusion model. Moreover, its specific mechanism is the activation of the Rac-1. The damage of increased ROS to blood brain barrier after cerebral ischemia and reperfusion has been widely reported and confirmed [7, 8, 53]. ROS destroy the BBB not only by influencing the MMP-9 and TJ proteins but also by directly influencing the endothelial cell. Hence, fibulin-5 has the role of rescuing vascular endothelial cells from apoptosis and alleviating BBB damage.

There are several limitations in the present study. First, the potential protective effect of fibulin-5 to oxidative stress after I/R was only tested under the condition of overexpression. Second, the fibulin-5-controlled ROS production was achieved by the activation of Rac-1 after I/R; other mechanisms remains unclear. Building on the present study of the SOD, it is necessary to determine the role of ecSOD under the intervention and the downstream mechanism of the integrin pathway in the future.

In conclusion, the present study investigated the mechanisms of neuro-protection following I/R. The results of present study show that the increased expression of fibulin-5 following cerebral ischemia reperfusion plays an important role in controlling ROS production, reducing brain cell apoptosis and vessel endothelial cells and BBB extravasation. Fibulin-5 may also play a role in adjusting the oxidative stress status, which opens a new window in the study of antioxidant mechanisms underlying cerebral ischemia reperfusion.

References

1. Kaushal V, Schlichter LC (2008) Mechanisms of microglia-mediated neurotoxicity in a new model of the stroke penumbra. J Neurosci 28(9):2221–2230
2. Yang Y, Rosenberg GA (2011) Blood-brain barrier breakdown in acute and chronic cerebrovascular disease. Stroke 42:3323–3328
3. Khatri R, McKinney AM, Swenson B, Janardhan V (2012) Blood-brain barrier, reperfusion injury, and hemorrhagic transformation in acute ischemic stroke. Neurology 79:S52–S57
4. Kahles T, Luedike P, Endres M, Endres M, Galla HJ, Steinmetz H, Busse R, Neumann-Haefelin T et al (2007) NADPH oxidase plays a central role in blood-brain barrier damage in experimental stroke. Stroke 38(11):3000–3006
5. Kamada H, Yu F, Nito C, Chan PH (2007) Influence of hyperglycemia on oxidative stress and matrix metalloproteinase-9 activation after focal cerebral ischemia/reperfusion in rats. Stroke 38(3):1044–1049
6. Paravicini TM, Touyz RM (2006) Redox signaling in hypertension. Cardiovasc Res 71(2):247–258
7. Szocs K (2004) Endothelial dysfunction and reactive oxygen species production in ischemia/reperfusion and nitrate tolerance. Gen Physiol Biophys 23(3):265–295
8. Haorah J, Ramirez SH, Schall K, Smith D, Pandya R, Persidsky Y (2007) Oxidative stress activates protein tyrosine kinase and matrix metalloproteinases leading to blood-brain barrier dysfunction. J Neurochem 101(2):566–576
9. Liu Y, Wang D, Wang H, Qu Y, Xiao X, Zhu Y (2014) The protective effect of HET0016 on brain edema and blood-brain barrier dysfunction after cerebral ischemia/reperfusion. Brain Res 1544:45–53
10. Pun PB, Lu J, Moochhala S (2009) Involvement of ROS in BBB dysfunction. Free Radic Res 43:348–364
11. Dirnagl U (2012) Pathobiology of injury after stroke: the neurovascular unit and beyond. Ann N Y Acad Sci 1268:21–25
12. Williamson MR, Shuttleworth A, Canfield AE, Black RA, Kielty CM (2007) The role of endothelial cell attachment to elastic fibre molecules in the enhancement of monolayer formation and retention, and the inhibition of smooth muscle cell recruitment. Biomaterials 28(35):5307–5318
13. Yanagisawa H, Schluterman MK, Brekken RA (2009) Fibulin-5, an integrin-binding matricellular protein: its function in development and disease. J Cell Commun Signal 3(3–4):337–347
14. Schiemann WP, Blobe GC, Kalume DE, Pandey A, Lodish HF (2002) Context-specific effects of fibulin-5 (DANCE/EVEC) on cell proliferation, motility, and invasion. Fibulin-5 is induced by transforming growth factor-beta and affects protein kinase cascades. J Biol Chem 277(30):27367–27377
15. Albig AR, Neil JR, Schiemann WP (2006) Fibulins 3 and 5 antagonize tumor angiogenesis in vivo. Cancer Res 66(5):2621–2629
16. Yue W, Sun Q, Landreneau R, Wu C, Siegfried JM, Yu J, Zhang L (2009) Fibulin-5 suppresses lung cancer invasion by inhibiting matrix metalloproteinase-7 expression. Cancer Res 69(15):6339–6346
17. MØller HD, Ralfkjær U, Cremers N, Frankel M, Pedersen RT, Klingelhöfer J, Yanagisawa H, Grigorian M et al (2011) Role of fibulin-5 in metastatic organ colonization. Mol Cancer Res 9(5):553–563
18. Kowal RC, Richardson JA, Miano JM, Olson EN (1999) EVEC, a novel epidermal growth factor-like repeat-containing protein upregulated in embryonic and diseased adult vasculature. Circ Res 84(10):1166–1176
19. Spencer JA, Hacker SL, Davis EC, Mecham RP, Knutsen RH, Li DY, Gerard RD, Richardson JA et al (2005) Altered vascular remodeling in fibulin-5-deficient mice reveals a role of fibulin-5 in smooth muscle cell proliferation and migration. Proc Natl Acad Sci U S A 102(8):2946–2951
20. Guadall A, Orriols M, Rodríguez-Calvo R, Calvayrac O, Crespo J, Aledo R, Martínez-González J, Rodríguez C (2011) Fibulin-5 is up-regulated by hypoxiain endothelial cells through a hypoxia-inducible factor-1 (HIF-1)-dependent mechanism. J Biol Chem 286(9):7093–7103
21. Kapustin A, Stepanova V, Aniol N, Cines DB, Poliakov A, Yarovoi S, Lebedeva T, Wait R et al (2012) Fibulin-5 binds urokinase-type plasminogen activator and mediates urokinase stimulated β1-integrin-dependent cell migration. Biochem J 443(2):491–503
22. Schluterman MK, Chapman SL, Korpanty G, Ozumi K, Fukai T, Yanagisawa H, Brekken RA (2010) Loss of fibulin-5 binding to beta1 integrins inhibits tumor growth by increasing the level of ROS. Dis Model Mech 3(5–6):333–342
23. Li L, Liu F, Welser-Alves JV, McCullough LD, Milner R (2012) Upregulation of fibronectin and the α5β1 and αvβ3 integrins on blood vessels within the cerebral ischemic penumbra. Exp Neurol 233(1):283–291
24. Milner R, Hung S, Erokwu B, Dore-Duffy P, LaManna JC, del Zoppo GJ (2008) Increased expression of fibronectin and the alpha 5 beta 1 integrin in angiogenic cerebral blood vessels of micesubject to hypobaric hypoxia. Mol Cell Neurosci 38(1):43–52
25. Nguyen AD, Itoh S, Jeney V, Yanagisawa H, Fujimoto M, Ushio-Fukai M, Fukai T (2004) Fibulin-5 is a novel binding protein for extracellular superoxide dismutase. Circ Res 95(11):1067–1074
26. Reed LJ, Muench H (1938) A simple method of estimating fifty per cent endpoint. Am J Hyg 27:493–497
27. Zhao LR, Duan WM, Reyes M, Keene CD, Verfaillie CM, Low WC (2002) Human bone marrow stem cells exhibit neural phenotypes and ameliorate neurological deficits after grafting into the ischemic brain of rats. Exp Neurol 174(1):11–20
28. Zhang S, Zhang Q, Zhang JH, Qin X (2008) Electro-stimulation of cerebellar fastigial nucleus (FNS) improves axonal regeneration. Front Biosci 13:6999–7007
29. Feng J, Wang T, Li Q, Wu X, Qin X (2012) RNA interference against repulsive guidance molecule A improves axon sprout and neural function recovery of rats after MCAO/reperfusion. Exp Neurol 238(2):235–242
30. Zhang J, Takahashi HK, Liu K, Wake H, Liu R, Maruo T, Date I, Yoshino T et al (2011) Anti-high mobility group box-1 monoclonal antibody protects the blood-brain barrier from ischemia-induced disruption in rats. Stroke 42(5):1420–1428
31. Hu Q, Chen C, Yan J, Yang X, Shi X, Zhao J, Lei J, Yang L et al (2009) Therapeutic application of gene silencing MMP-9 in a middle cerebral artery occlusion-induced focal ischemia rat model. Exp Neurol 216(1):35–46
32. Schober W (1986) The rat cortex in stereotaxic coordinates. J Hirnforsch 27(2):121–143
33. Kawamata T, Speliotes EK, Finklestein SP (1997) The role of polypeptide growth factors in recovery from stroke. Adv Neurol 73:377–382
34. Hunter AJ, Hatcher J, Virley D, Nelson P, Irving E, Hadingham SJ, Parsons AA (2000) Functional assessments in mice an drats after focal stroke. Neuropharmacology 39(5):806–816
35. Yu YS, Sui HS, Han ZB, Li W, Luo MJ, Tan JH (2004) Apoptosis in granulosa cells during follicular atresia: relationship with steroids and insulin-like growth factors. Cell Res 14(4):341–346

36. Wang X, Sugimoto K, Fujisawa T, Shindo N, Minato S, Kamada Y, Hamano M, Ohishi M et al (2014) Novel effect of ezetimibe to inhibit the development of non-alcoholic fatty liver disease in Fatty Liver Shionogi mouse. Hepatol Res 44(1):102–113
37. Zhang QG, Wang R, Han D, Dong Y, Brann DW (2009) Role of Rac1 GTPase in JNK signaling and delayed neuronal cell death following global cerebral ischemia. Brain Res 1265:138–147
38. Chiarugi P, Pani G, Giannoni E, Taddei L, Colavitti R, Raugei G, Symons M, Borrello S et al (2003) Reactive oxygen species as essential mediators of cell adhesion: the oxidative inhibition of a FAK tyrosine phosphatase is required for cell adhesion. J Cell Biol 161(5):933–944
39. Jean JC, Eruchalu I, Cao YX, Joyce-Brady M (2002) DANCE in developing and injured lung. Am J Physiol Lung Cell Mol Physiol 282(1):L75–L82
40. Kuang PP, Goldstein RH, Liu Y, Rishikof DC, Jean JC, Joyce-Brady M (2003) Coordinate expression of fibulin-5/DANCE and elastin during lung injury repair. Am J Physiol Lung Cell Mol Physiol 85(5):L1147–L1152
41. Lee MJ, Roy NK, Mogford JE, Schiemann WP, Mustoe TA (2004) Fibulin-5 promotes wound healing in vivo. J Am Coll Surg 199(3): 403–410
42. Osada T, Gu YH, Kanazawa M, Tsubota Y, Hawkins BT, Spatz M, Milner R, del Zoppo GJ (2011) Interendothelial claudin-5 expression depends on cerebral endothelial cell–matrix adhesion by b1-integrins. J Cereb Blood Flow Metab 31(10):1972–1985
43. Lim ST, Esfahani K, Avdoshina V, Mocchetti I (2011) Exogenous gangliosides increase the release of brain-derived neurotrophic factor. Neuropharmacology 60(7–8):1160–1167
44. Mahanivong C, Krüger JA, Bian D, Reisfeld RA, Huang S (2006) A simplified cloning strategy for the generation of an endothelial cell selective recombinant adenovirus vector. J Virol Methods 135(1):127–135
45. Shyu WC, Lin SZ, Chiang MF, Ding DC, Li KW, Chen SF, Yang HI, Li H (2005) Overexpression of PrPC by adenovirus-mediated gene targeting reduces ischemic injury in a stroke rat model. J Neurosci 25(39):8967–8977
46. Ayata C, Ropper A (2002) Ischaemic brain oedema. J Clin Neurosci 9:113–124
47. Nakamura T, Lozano PR, Ikeda Y, Iwanaga Y, Hinek A, Minamisawa S, Cheng CF, Kobuke K et al (2002) Fibulin-5/DANCE is essential for elastogenesis in vivo. Nature 415(6868): 171–175
48. Preis M, Cohen T, Sarnatzki Y, Ben Yosef Y, Schneiderman J, Gluzman Z, Koren B, Lewis BS et al (2006) Effects of fibulin-5 on attachment, adhesion, and proliferation of primary human endothelial cells. Biochem Biophys Res Commun 348(3):1024–1033
49. Lomas AC, Mellody KT, Freeman LJ, Bax DV, Shuttleworth CA, Kielty CM (2007) Fibulin-5 binds human smooth-muscle cells through alpha5beta1 and alpha4beta1 integrins, but does not support receptor activation. Biochem J 405(3):417–428
50. Woo CH, Eom YW, Yoo MH, You HJ, Han HJ, Song WK, Yoo YJ, Chun JS et al (2000) Tumor necrosis factor-alpha generates reactive oxygen species via a cytosolic phospholipase A2-linked cascade. J Biol Chem 275(41):32357–32362
51. del Pozo MA, Price LS, Alderson NB, Ren XD, Schwartz MA (2000) Adhesion to the extracellular matrix regulates the coupling of the small GTP-ase Rac to its effector PAK. EMBO J 9(9):2008–2014
52. Brakebusch C, Bouvard D, Stanchi F, Sakai T, Fassler R (2002) Integrins in invasive growth. J Clin Invest 109:999–1006
53. Lehner C, Gehwolf R, Tempfer H, Krizbai I, Hennig B, Bauer HC, Bauer H (2011) Oxidative stress and blood-brain barrier dysfunction under particular consideration of matrix metalloproteinases. Antioxid Redox Signal 15(5):1305–1323